2015 VESPUCCI INSTITUTE
Article submitted for review

Analysis of dynamic radiation level changes using surface networks

Myeong-Hun Jeong[1], Shaowen Wang[1], and Clair J. Sullivan[2]

[1]CyberGIS Center for Advanced Digital and Spatial Studies
CyberInfrastructure and Geospatial Information Laboratory
Department of Geography and Geographic Information Science
National Center for Supercomputing Applications, University of Illinois at Urbana-Champaign, Champaign, IL, 61820, USA
[2]Department of Nuclear, Plasma, and Radiological Engineering, University of Illinois at Urbana-Champaign, Champaign, IL, 61820, USA

November 9, 2015

Abstract: The Fukushima nuclear accident reminds us of severe risk of radioactive substances. Citizen scientists voluntarily collect and share radiation data using geo-tagged sensors for radiation preparedness. However, radiation levels are affected by a number of factors including for example weather conditions, naturally occurring radioactive materials (NORM), and large marble structures. It is therefore difficult to determine whether a higher radiation level comes from a normal variation in background or not. This research analyzes the radiation changes using surface networks that can be used to characterize complex surfaces. A new algorithm has been developed to identify salient peaks and their hills by merging insignificant peaks recursively. Salient peaks and their hills are converted into graphs. The structural similarities of graphs were compared over time. The radiation measurements in the city of Koriyama, Japan were analyzed as a case study. The results demonstrated that structural analysis of dynamic radiation levels revealed stable changes, while numeric analysis of radiation levels presented statistically significant differences. This method is able to detect radiation level changes irrespective of background variations.

Keywords: surface networks, structural similarities, graph indices, radiation levels

1 Introduction

Radiation levels have been a subject of major debate after a nuclear disaster – Fukushima Daiichi accident – released substantial contamination into our environments. Citizen scientists, as it came to be known, started gathering and sharing environmental radiation levels using mobile detectors (e.g., Geiger counters) across the world due to awareness of health effects. In particular, the non-profit organization such as Safecast has been building a radiation sensor network from crowd-sourced data. Its data points have been over 25 million at the end of 2014 [1].

While an immense number of radiation sensors quantify the levels of radiation in our environment, it is difficult to understand accurate radiation levels due to background variations [29, 18]. For example, some regions have naturally occurring radioactive materials (NORM); weather such as precipitation causes the increase of background levels, or background levels have a tendency to increase as a result of the presence of large marble structures. It is challenging to predict whether the amplitude of the count rate is due to the possible release of radioactive materials or not.

However, looking beyond direct background effects on radiation levels, this paper investigates how the structure of regions of higher count rates have changed as time varies. We assume if radioactive materials are continually stable, the structure of the regions of higher count rates would have similar patterns, irrespective of background fluctuations. In this paper, the regions of higher count rates are represented by surface networks, consisting of critical points (peaks, pits, and passes) and critical lines (ridges and channels) [24, 25]. We particularly focus on salient peaks and their hills such as catchments areas. Salient peaks are connected by edges. Such a graph between subsequent time steps have been analyzed and compared using graph structural analysis techniques [26]. The structural analysis can provide dynamic radiation level changes without knowing accurate background variations.

In the reminder, the following section starts by discussing the previous computations of surface networks and structural similarity measurements between surface networks. Section 3 describes the data processing for parsing and filtering radiation data set. Section 4 provides a surface network algorithm presented in this study. In addition, this section provides the information about analysis methods. Section 5 presents evaluations of structural analysis. The results confirm the effectiveness of the approach, discussed in Section 6. Finally, the conclusions and future works are drawn in Section 7.

2 Background

This paper utilizes spatial reasoning for identifying radiation level changes. The radiation level changes may be identified by using cluster analysis from a group of radiation measurements. However, it is difficult to separate radiation measurements appropriately because radiation levels are floating at even the same location due to background

effects.

In this paper, radiation measurements are converted to raster maps. The radiation scalar fields (i.e., raster maps) are characterized by surface networks. The regions of higher count rates are represented as peaks and their hills on the surface network. The structural similarity of surface networks are compared in order to infer radiation level changes.

Surface networks originate from the work of [6, 17], which do not describe the Earth's surface as hills and valley, but also propose relations between the number of peaks, pits, and passes. In a later, Morse theory uses differential topology generally to define surface networks [19]. Morse theory pertains to the relationship between the shape of the space and functions on defined on the space. If the derivative of a height function $z = f(x, y)$ equals to zero at a point (x_0, y_0), this point (x_0, y_0) is called a critical point, if and only if the determinant of the Hessian matrix $\left(\begin{smallmatrix} f_{xx}(x_0,y_0) & f_{xy}(x_0,y_0) \\ f_{yx}(x_0,y_0) & f_{yy}(x_0,y_0) \end{smallmatrix}\right)$ is not zero, where $f_{xx}, f_{xy}, f_{yx}, f_{yy}$ are partial derivatives of the height function, z [16].

There are broadly two approaches to construct surface networks from continuous surfaces to discrete data structures: explicit and implicit cell complexes.

Explicit cell complexes can be regarded as triangulations. The critical points are extracted from the triangular mesh by comparing values with adjacent points [30] or piecewise linear functions [10, 8]. Illicit cell complexes make use of a grid such as raster-based DEMs [23, 35]. We use a grid configuration of each radiation measurements (i.e., a raster map). In particular, we focus on the detection of peaks and their hills because our purpose is to identify regions of higher count rates. The hills of peaks are called as Morse complexes [8]. One example for using Morse complex is to analyze and track burning structures [3].

Based on a raster map, there are several ways to identify critical points. [23] use local comparisons between eight direct neighbors. Local comparisons are known to identify spurious critical points due to continuity constraints [27]. [34, 35] uses biquadratic interpolation as well as geomorphological parameters, which help to remove spurious critical points. However, geomorphological parameters (e.g., slope and curvature) can not guarantee that all peaks are identified due to the violation of geomorphological parameters' constraints, although geomorphological approach is good at removing spurious critical points. The regions of higher does rates are important in our application. In such context, this paper presents a new algorithm for identifying salient critical points (i.e., peaks) in a radiation scalar field using prominence (i.e., the relative height difference between adjacent peaks) and horizontal distance (i.e., distance between adjacent peaks). Our approach recursively removes insignificant peaks.

In terms of measuring similarity between surface networks, there is very few research on the structural analysis of surface networks. One example is to calculate structural similarity index for the analysis of urban population surfaces [21]. In the first step, identified surface networks are generalized by removing peaks that have the minimum difference in height with associated passes. Critical points are then sorted

based on the height. Sorted critical points are continually deleted until there is only one peak left. During this process, structural similarity index is given if two surface networks are isomorphic. However, this approach is ill-suited to our problem in the sense that background fluctuations lead to different radioactive levels in spite of the same count rates in reality.

Another approach is to use graph theoretic indices (e.g., density or connectivity) to analyze the surface and its changes over time [12]. However, graph theoretic indices are not enough to characterize radiation level changes because a network connectivity can be different without significant radiation level changes. None of approaches encountered are directly applicable to our problems. Therefore we adapt graph similarity measurement techniques for quantifying the similarity of surface networks. There are a broad range of applications in graph similarity scoring and matching techniques: chemical structures [14, 32], social media [5, 20], web searching [2, 9] or medical diagnostics [28].

In summary, this paper provides a new algorithm to identify salient peaks among spurious peaks. In addition, the structural similarity of surface and its changes are measured using graph similarity scoring and measuring techniques. We demonstrate that this approach can provide global radiation level changes without accurate background measurements.

3 Data processing

Based on our previous literature review, we will now proceed with data processing for the analysis of radiation level changes. We acquired experimental radiation data set from Safecast in February, 2015. The data size is over 26 million records and over 3 GB as a csv file format.

The experimental area was selected in Japan because citizen scientists have been gathering substantial numbers of radiation measurements across Japan. Our experimental region is the city of Koriyama that is $82km$ away from Fukushima Daiichi nuclear power station (i.e., WGS84 bounds are 140.32564, 37.36191, 140.40993, 37.43678). We gathered all measurements each month in 2013. Thus, there are twelve data set for the city of Koriyama.

In order to analyze a large volume of data, we exploited Apche Pig and Hadoop. The former is a programming language designed to ease the development of distributed applications for analyzing large volumes of data. The later can be thought of distributed computing framework designed for processing large distributed data [22]. By using Pig and Hadoop, we can derive experimental data set with ease and speed.

Finally, all measurements per month are converted into raster maps using Empirical Bayesian Kriging (EBK). EBK is well known to have smaller prediction uncertainty and the ability to filter out measurement errors [15]. These interpolation maps have been used as the cornerstone for identifying surface networks as well as analyzing

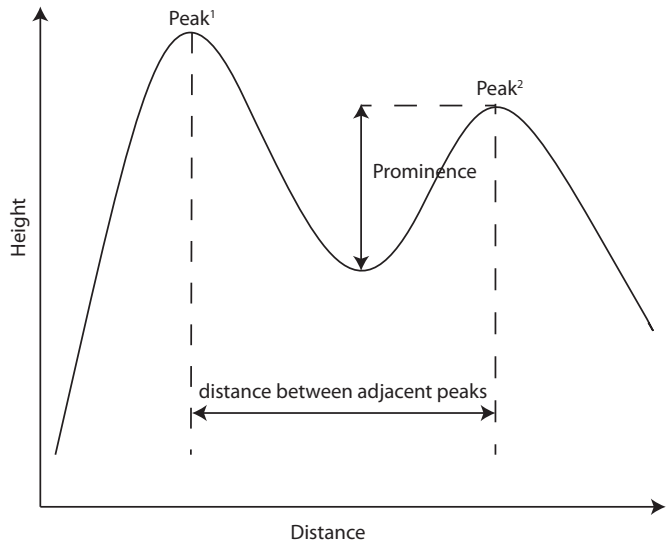

Figure 1: Prominence and horizontal distance between Peak^1 and Peak^2. This figure is adapted from [7].

radiation level changes.

4 Surface networks

In this section, we explore a new algorithm to identify peaks and their hills in a radiation scalar field. Further, the analysis methods are presented: how well surface networks reflect the radiation measurements; numerical summaries of surface networks' structure; and structural similarity of surface and its changes over time.

4.1 Identification of peaks and hills

In order to explain an algorithm, it is necessary to mention basic definitions related with critical points.

In brief, a peak, *pk* is defined as a cell that all neighbors of *pk* have a lower value than *pk*. The ascent vector, *av* of an each cell is defined as the unique directed edge from that cell to its one-hop neighbor with the highest value of all neighbors. Prominence, *prom* is described as relative height difference between adjacent peaks. These basic definitions have been already defined by previous works [30, 13, 7]. In addition, we can add another definition such as a horizontal distance, *hd* between adjacent peaks. Prominence and horizontal distance are mainly used to remove spurious peaks in our algorithm. Figure 1 illustrates prominence and horizontal distance.

Based on definitions mentioned above, the algorithm proceeds as follows:

- Each cell decides its ascent vector by comparing values with direct eight neighbors (Algorithm 1, line 7). If a cell has the highest value among neighbors, this cell becomes a peak (Algorithm 1, line 4)
- Each peak broadcasts top-down sweep messages to neighbors. Each cell updates its peak identifier, *pkid* based on its *av*'s peak identifier (Algorithm 1, line 9). During this process, if there are neighbors that have a different peak identifier, this cell becomes a channel (i.e., the direction of ascent vectors are divided at channels into different peaks).
- Peaks are recursively merged using prominence and horizontal distance (Algorithm 1, line 11).
- All cells' peak identifier will be updated and reconciled if a cell has an disappeared peak identifier (Algorithm 1, line 17).

Algorithm 1 Identifying peaks and their hills

1: Input: Raster-based radiation grid, *prom*: user defined prominence threshold, *hd*: user defined horizontal distance threshold
2: Local variables: an ascent vector, *av*, initialized empty; a peak id, *pkid*, initialized empty

Step I
3: Comparing radiation values with direct 8 neighbors
4: **if** a cell has the highest value among neighbors **then**
5: this cell becomes a local peak (*pk*) *--local comparisons between direct 8 neighbors*
6: **else**
7: **set** *av* := one of neighbors' peak identifier that has the highest value

Step II
8: Top-down sweep from local peaks
9: **set** *pkid* := *av*'s peak identifier

Step III
10: Remove insignificant peaks *--Considering all identified peaks*
11: **if** peaks are adjacent to each other **then** *--There are channels between two peaks*
12: **if** relative height $<$ *prom* **then**
13: **if** horizontal distance $< 1.5 \times$ IQR and horizontal distance $<$ *hd* **then**
14: **set** *pkid* := adjacent peak's identifier *--If there are no more two adjacent peaks, we use a default horizontal distance*

Step IV
15: Merge peaks and hills
16: **if** an insignificant peak identifier is merged into a new peak identifier **then**
17: **set** *pkid* := new peak's identifier *--Update a peak identifier if a cell has an disappeared peak identifier*

In particular, step III can remove spurious peaks. There are two steps. First, if the relative height between adjacent peaks meets a threshold prominence, a peak that has a lower height will be merged into another peak. Thus, we can generalize the surface networks if a radiation difference is negligible. This is a similar approach of

Wolf pruning [33] in terms of simplifying surface networks using relative height. Next, each peak has usually several adjacent peaks. When we repeat the merge process, we consider the distance between adjacent peaks because spatially near measurements are more related. If a horizontal distance between adjacent peaks is far away compared with other adjacent peaks (i.e., horizontal distance $> 1.5\times$ interquartile ranges (IQR)), the algorithm does not merge adjacent two peaks. The interquartile ranges can be calculated with distances from other adjacent peaks. If there are only two peaks such as a very smooth field, we can use a user defined threshold distance.

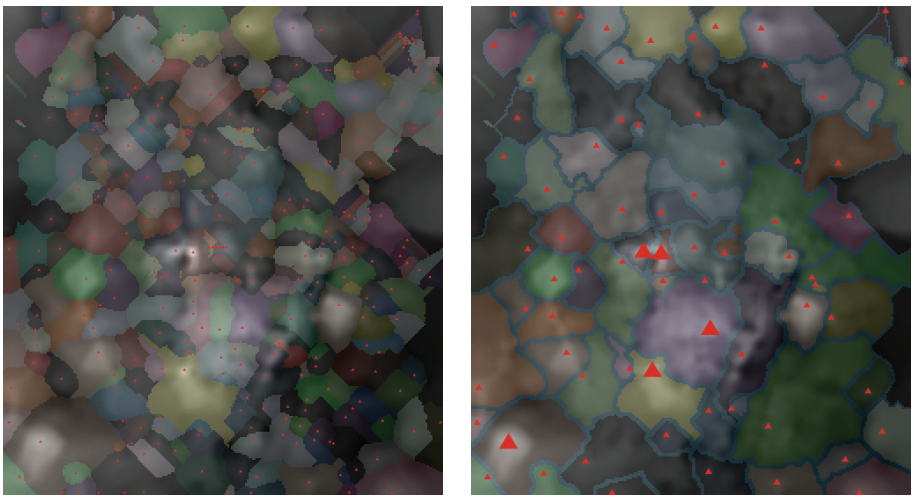

(a) Initial identified peaks and hills (b) Salient peaks and hills

Figure 2: Identification of salient peaks and hills at Koriyama in May 2013

Figure 2 presents how the initial identified peaks are merged into salient peaks. 317 peaks are initially identified in Figure 2a. The number of peaks are then reduced to 73 in Figure 2b. In addition, Top 5 representative peaks are highlighted using bigger triangle symbols in Figure 2b. These peaks and hills are main interest in our radiation level analysis (see Section 5).

4.2 Analysis techniques

Three analysis methods are exploited in this paper: feature based parameters for analyzing the correlation between identified surface networks and radiation measurements; graph indices, and graph structural similarity for comparing surface networks over time.

First, identified surface networks were measured using feature based parameters. There are a couple of feature based parameters, including the absolute peak height, the peak area, the peak volume, the peak curvature in sliding direction, or the peak density per unit area. These feature parameters have been used to understand the

surface functional performance in nanotechnology [11, 31]. We will use the absolute peak height to measure the relationship between feature based parameters and the numeric calculations of radiation measurements. If the radiation measurements are reflected in the identified surface networks, the feature based parameters correlate well with the radiation measurements.

Next, surface networks were distilled based on graph theory. Graph indices can provide succinct numerical summaries of the network structure [12]. Graph density and connectedness are used to describe the network structure in this paper. In brief, the density refers to the number of observed edges over the number of possible ones. The connectedness indicates whether there exists an undirected path from a node u to a node v in a graph [26]. If both values equal to one, the regions of high count rates are densely clustered.

Lastly, we can analyze the surface network and its changes over time using structural similarities. The basic idea is to establish a matching between the edges of one graph and the edges of another using density [4]. The structural correlation can be derived from structural comparison measures. For example, if the structural correlation $= 1$, the graphs are isomorphic. We use the SNA R package to calculate structural correlation. This package provides a wide range of graph analytic functionalities [5].

Analysis methods mentioned above were experimentally conducted and tested in the following section.

5 Results

The following section started by investigating the numerical analysis of the raw radiation measurements. The algorithm described in the previous section was evaluated with the relationship between feature based parameters and numerical analysis of radiation measurements. In order to measure radiation level changes, the structural variations of surface networks over time were analyzed with graph indices and structural similarity correlations.

5.1 Numerical data analysis

Figure 3 presents the spread of radiation measurements. It is clear that there was a significance difference for each measurement. This visual impression was confirmed using statistical analysis, which is to find whether there is a statistically significant difference in radiation levels between each month.

As you may expect, the data violated the normal distribution assumption ($F(11, 510299) = 1048.5$, $p < 0.05$). Robust alternative one-way ANOVA test (i.e., Kruskal-Wallis test) was used for non-normal distributions. There was a statistically significant difference between each month ($H(11) = 48220.16$, $p = 2.2e - 16$). We conducted a follow-up analysis such as pairwise comparisons using Wilcoxon rank sum test to present which dependent variables (i.e., month) show a significant difference.

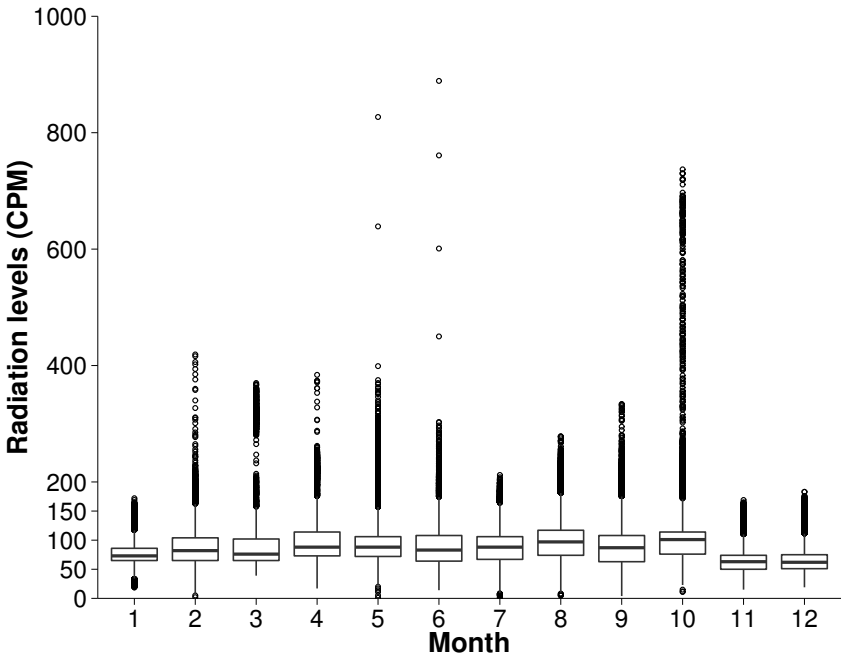

(a) The city of Koriyama, Japan in 2013

Figure 3: Boxplot of radiation levels split by month: 7 measurements over 1000 cpm were removed from the figure.

There were no significant differences between February and June, and February and September ($p > 0.05$), while presenting significant differences on other cases.

However, it is difficult to mention that there were significant differences in radiation levels in the city of Koriyama in 2013. These significant differences may be due to background variations such as precipitations. Further, there is not enough information to quantify background effects on the radiation levels, which makes it difficult to understand the real changes of radiation levels. Therefore, the following sections investigate the dynamic radiation levels using spatial structures of surface networks.

5.2 Feature based parameter analysis

Feature based parameters can provide information about how identified surface networks reflect the original radiation measurements. The feature based parameters (i.e., the average of absolute height) were calculated from the top 5 representative peaks in Table 1.

The correlation between the average of absolute height and the mean of radiation measurements was analyzed using Pearson's correlation coefficients, r. The null hypothesis is that there is a no correlation between feature based parameters and the mean of radiation measurements. The result indicated that the average of abso-

Table 1: Results for the mean of radiation measurements and the average of absolute height of top 5 representative peaks per month in 2013 (The unit is cpm).

	1	2	3	4	5	6	7	8	9	10	11	12
Mean	77.23	91.75	91.53	100.9	93.31	88	88.31	96.32	87.55	102.9	64.15	66.38
Height	149.71	166.70	156.42	163.88	178.21	159.26	145.19	172.93	158.04	215.55	134.97	149.58

lute height was significantly related to the increase of the radiation levels, $r = 0.74$, $p = 0.004$. In terms of effect sizes, the correlation coefficient, r is greater than 0.5. It can be interpreted as a large effect. Therefore, the radiation levels are appropriately reflected in the surface networks.

5.3 Structural indices analysis of surface networks

Surface networks are naturally a graph. The regions of higher count rates are of interest in our application. These regions can be represented by peaks and their hills. Since the regions with very high radiation levels are meaningful, we only considers the top 5 representative peaks. These salient peaks are extracted to form an undirected graph. For example, in Figure 2b, the top 5 representative peaks are converted into a undirected graph by connecting adjacent peaks in Figure 4a. This graph is also represented as an adjacency matrix in Figure 4b. These adjacency matrix can be used as the basis for graph indices and similarity analysis.

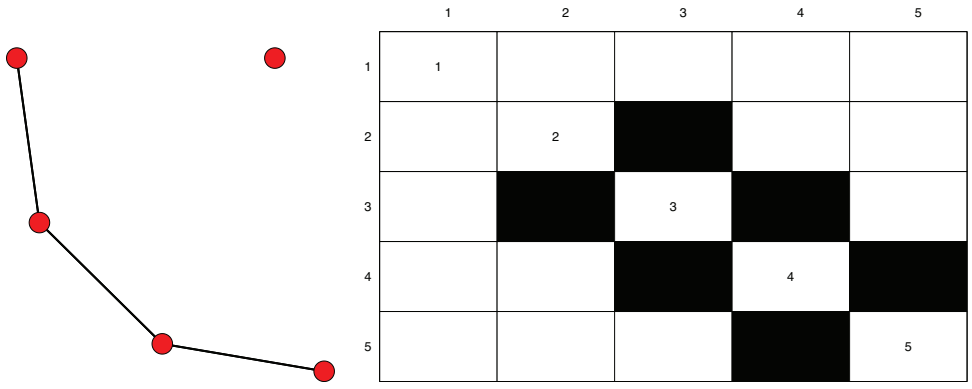

(a) Undirected graph (b) Adjacency matrix

Figure 4: Undirected graph and its adjacency matrix for the top 5 salient peaks in Figure 2b.

Surface networks in every month were converted into undirected graphs. These graphs were analyzed with graph indices and connectedness measurements in Figure 5a.

If you look at the density, most values of density were lower values, which indi-

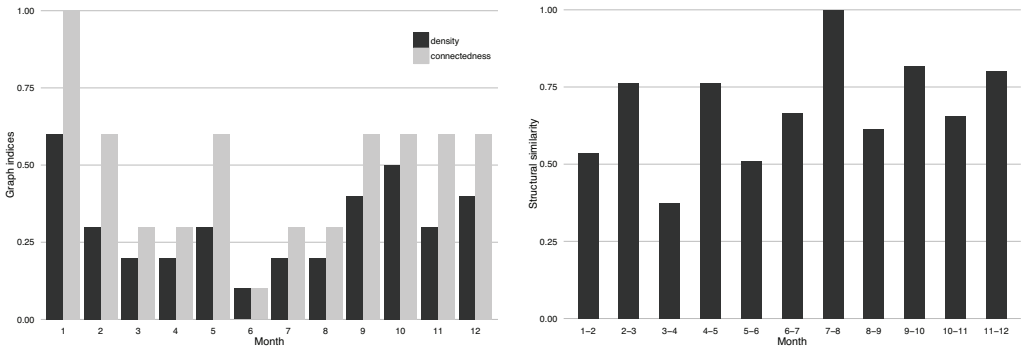

(a) Density and connectedness (b) Structural similarity

Figure 5: Graph indices and structural similarities

cated a sparsely connected graph. Further, the value of connectedness indicated there was a isolated node (i.e., a peak and its hill) except January. However, these graph indices are not related with radiation level changes. In other words, as the mean of radiation levels increase, the graph indices are not correlated. We can just quantitatively summarize the structure of a graph per month. Thus, the following section compared the structure similarity of graphs associated with the mean of radiation levels.

5.4 Structural similarity analysis of surface networks

An important alternative to graph indices is a direct comparison of edges sets between two graphs. The structural correlations between two graphs were calculated for measuring structural similarity.

Results for the structural correlations over time are represented in Figure 5b. For example, the first bar indicates the structural correlation between January and February, 0.54.

Overall, the structural similarities were fairly correlated except between March and April. These results are a total contrast to the numeric analysis in Section 5.1. Even though there is no information about accurate background effects, it is available to infer how radiation levels have changed using structural similarities of surface networks.

6 Discussion

Our numerical analysis of radiation measurements demonstrated that there were statistically significant differences between each month in terms of radiation levels. However, it is difficult to understand whether this difference comes from radioactive materials release or background fluctuations.

In terms of the feature based parameters analysis, the identified surface networks well reflected the radiation measurements. The correlation coefficients, r between the average of absolute height and the mean of radiation measurements was greater 0.7. This can be regarded as large effect size. Further, this feature based parameter was significantly correlated to the radiation measurements ($p < 0.05$). However, the computational analysis of the algorithm proposed was not conducted in this research because this paper focused on the analysis of radiation level changes.

When it comes to structural indices analysis, we can quantitatively summarize the structure of radiation levels per month. Using structural indices, it can be inferred whether the regions of higher count rates are highly clustered or separated per month. However, it is difficult to determine radiation level changes using graph indices.

The last evaluation criteria was the structural similarity analysis. The structural correlations presented that there were fair correlations for the radiation level changes over time. This result confirmed that the variations of radiation levels were attributed to background fluctuations rather than radioactive contamination. However, the structural similarities were not exactly the same each month. Some parts of salient regions had been changed per month. This work should be incorporated into research on principal component analysis such as precipitation, or wind. In addition, the structural similarity just provides the correlation coefficient. It is difficult to infer what kinds of topological events occur between subsequent time steps. Tree morphism and Homology algorithm could be exploited to detect qualitative topological events of radiation level changes.

7 Conclusions

This paper has demonstrated how radiation level changes can be identified using the structural similarities of surface networks. The structural similarities over time provide fair correlations for the radiation level changes, even though the numerical analysis indicates there are statistically significant differences for radiation levels.

The approach presented in this paper has taken a key step in addressing background effects in radioactive engineering. This research is part of a larger project to detect the illicit movement of nuclear materials with big data. The structural analysis can be used efficiently to monitor illicit nuclear materials, irrespective of background fluctuations.

Acknowledgments

This work was supported in part by the U.S. National Science Foundation (grant numbers: 0846655, 1047916, and 1443080) and the Defense Advanced Research Projects Agency (grant number: N66001-14-1-4043). The views, opinions, and findings contained in this article are those of the authors and should not be interpreted as repre-

senting the official views or policies, either expressed or implied, of the National Science Foundation, the Defense Advanced Research Projects Agency or the Department of Defense.

References

[1] Safecast. http://blog.safecast.org. [Online; accessed 04-March-2015].

[2] BLONDEL, V. D., GAJARDO, A., HEYMANS, M., SENELLART, P., AND VAN DOOREN, P. A measure of similarity between graph vertices: Applications to synonym extraction and web searching. *SIAM review 46*, 4 (2004), 647–666.

[3] BREMER, P., WEBER, G., PASCUCCI, V., DAY, M., AND BELL, J. Analyzing and tracking burning structures in lean premixed hydrogen flames. *IEEE Transactions on Visualization and Computer Graphics 16*, 2 (2010), 248–260.

[4] BUTTS, C., AND CARLEY, K. Multivariate methods for interstructural analysis. Casos working paper, Carnegie Mellon University., 2001.

[5] BUTTS, C. T. Social network analysis with sna. *Journal of Statistical Software 24*, 6 (2008), 1–51.

[6] CAYLEY, A. On contour and slope lines. *Philosophical Magazine Series 4 18*, 120 (1859), 264–268.

[7] CHAUDHRY, O. Z., AND MACKANESS, W. A. Creating mountains out of mole hills: Automatic identification of hills and ranges using morphometric analysis. *Transactions in GIS 12*, 5 (2008), 567–589.

[8] DANOVARO, E., DE FLORIANI, L., PAPALEO, L., AND VITALI, M. A multi-resolution representation for terrain morphology. In *Geographic Information Science*, M. Raubal, H. Miller, A. Frank, and M. Goodchild, Eds., vol. 4197 of *Lecture Notes in Computer Science*. Springer, Berlin Heidelberg, 2006, pp. 33–46.

[9] DEHMER, M., STREIB, F. E., MEHLER, A., KILIAN, J., AND MÜHLHÄUSER, M. Application of a similarity measure for graphs to web-based document structures. In *International Conference on Data Analysis ICA* (2005).

[10] EDELSBRUNNER, H., HARER, J., AND ZOMORODIAN, A. Hierarchical Morse Smale complexes for piecewise linear 2 manifolds. *Discrete and Computational Geometry 30* (2003), 87–107.

[11] HAO, Q., BIANCHI, D., KAESTNER, M., AND REITHMEIER, E. Feature based characterization of worn surfaces for a sliding test. *Tribology International 43*, 5 (2010), 1186–1192.

[12] HU, Y., MILLER, H. J., AND LI, X. Detecting and analyzing mobility hotspots using surface networks. *Transactions in GIS 18*, 6 (2014), 911–935.

[13] JEONG, M.-H., DUCKHAM, M., MILLER, H., KEALY, A., AND PEISKER, A. Decentralized and coordinate-free computation of critical points and surface networks in a discretized scalar field. *International Journal of Geographical Information Science 28*, 1 (2014), 1–21.

[14] KAZIUS, J., NIJSSEN, S., KOK, J., BÄCK, T., AND IJZERMAN, A. P. Substructure mining using elaborate chemical representation. *Journal of Chemical Information and Modeling 46*, 2 (2006), 597–605.

[15] KRIVORUCHKO, K. *Spatial statistical data analysis for GIS users*. Esri Press Redlands, CA, USA, 2011.

[16] MATSUMOTO, Y. *An Introduction to Morse Theory*, vol. 208. American Mathematical Society, USA, 2002.

[17] MAXWELL, J. C. On hills and dales. *Philosophical Magazine Series 4 40* (1870), 421–427.

[18] MERCIER, J.-F., TRACY, B., D'AMOURS, R., CHAGNON, F., HOFFMAN, I., KORPACH, E., JOHNSON, S., AND UNGAR, R. Increased environmental gamma-ray dose rate during precipitation: A strong correlation with contributing air mass. *Journal of environmental radioactivity 100*, 7 (2009), 527–533.

[19] MILNOR, J. *Morse Theory*. Princeton University Press, 1969.

[20] MURATA, T., AND MORIYASU, S. Link prediction of social networks based on weighted proximity measures. In *IEEE/WIC/ACM international conference on Web Intelligence* (2007), IEEE, pp. 85–88.

[21] OKABE, A., AND MASUYAMA, A. A method for measuring structural similarity among activity surfaces and its application to the analysis of urban population surfaces in japan. In *Topological Data Structures for Surfaces : An Introduction for Geograhpical Information Science* (2004), S. Rana, Ed., Willey, pp. 103–120.

[22] PASUPULETI, P. *Pig Design Patterns*. Packt Publishing Ltd, 2014.

[23] PEUCKER, T. K., AND DOUGLAS, D. H. Detection of surface-specific points by local parallel processing of discrete terrain elevation data. *Computer Graphics and image processing 4*, 4 (1975), 375–387.

[24] PFALTZ, J. L. Surface networks. *Geographical Analysis 8*, 1 (1976), 77–93.

[25] RANA, S. *Topological Data Structures for Surfaces*. John Wiley & Sons, Ltd., Chichester, UK, 2004.

[26] SAMATOVA, N. F., HENDRIX, W., JENKINS, J., PADMANABHAN, K., AND CHAKRABORTY, A. *Practical Graph Mining with R*. CRC Press, 2013.

[27] SCHNEIDER, B., AND WOOD, J. Construction of metric surface networks from raster-based dems. In *Topological Data Structures for Surfaces : An Introduction for Geograhpical Information Science*, S. Rana, Ed. Willey, 2004, pp. 53–70.

[28] SHARMA, H., ALEKSEYCHUK, A., LESKOVSKY, P., HELLWICH, O., ANAND, R., ZERBE, N., AND HUFNAGL, P. Determining similarity in histological images using graph-theoretic description and matching methods for content-based image retrieval in medical diagnostics. *Diagn Pathol 7* (2012), 134.

[29] SULLIVAN, C. J. Nuclear forensics driven by geographic information systems and big data analytics. In *Proc. the Institute for Nuclear Materials Management on Information Analysis Technologies, Techniques and Methods for Safeguards, Nonproliferation and Arms Control Verification Workshop* (2014), pp. 273–286.

[30] TAKAHASHI, S., IKEDA, T., SHINAGAWA, Y., KUNII, T. L., AND UEDA, M. Algorithms for extracting correct critical points and constructing topological graphs from discrete geographical elevation data. *Computer Graphics Forum 14*, 3 (1995), 181–192.

[31] TIAN, Y., WANG, J., PENG, Z., AND JIANG, X. A new approach to numerical characterisation of wear particle surfaces in three-dimensions for wear study. *Wear 282* (2012), 59–68.

[32] WALE, N., WATSON, I. A., AND KARYPIS, G. Comparison of descriptor spaces for chemical compound retrieval and classification. *Knowledge and Information Systems 14*, 3 (2008), 347–375.

[33] WOLF, G. W. Knowledge diffusion from giscience to other fields: The example of the usage of weighted surface networks in nanotechnology. *International Journal of Geographical Information Science 28*, 7 (2014), 1401–1424.

[34] WOOD, J. *The geomorphological characterisation of digital elevation models*. PhD thesis, University of Leicester, 1996.

[35] WOOD, J. Modelling the continuity of surface form using digital elevation models. In *Proc. 8th international Symposium on Spatial Data Handling* (1998), IGU Commission of GIS New York, pp. 725–736.